Attempt to synthesize the proton-unbound ^{182,183}Bi isotopes

H. Huang,[1,2,3] H. Y. Wu,[4,5] C. Y. Guo,[5] W. Q. Zhang,[1,2] Q. B. Zeng,[1,2] D. X. Wang,[5] Z. Liu,[1,2,*] Z. H. Li,[5,†] A. N. Andreyev,[6,7,‡] S. Antalic,[8] B. Andel,[8] A. Sitarčík,[8] H. Hua,[5] X. H. Yu,[1,2] Z. X. Zhou,[5] X. Wang,[5] H. Y. Lu,[1,2] Z. G. Gan,[1,2] Z. Y. Zhang,[1,2] L. Ma,[1,2] M. H. Huang,[1,2] H. B. Yang,[1,2] M. M. Zhang,[1,2] X. J. Wen,[1] G. S. Li,[1,2] F. F. Zeng,[1,2] X. X. Xu,[1,2] J. J. Liu,[1,2] H. Jian,[1,2] H. F. Zhu,[1,2] Q. R. Gao,[1,2] Z. Qin,[1,2] J. R. Wang,[1,2] Z. M. Jia,[1,2] S. W. Cao,[1,2] P. F. Zhai,[1,2] Y. J. Li,[9] X. H. Zhou,[1,2] and F. S. Zhang[10,11]

[1]*Institute of Modern Physics, Chinese Academy of Sciences, Lanzhou 730000, China*
[2]*University of Chinese Academy of Sciences, Beijing 100049, China*
[3]*GSI Helmholtz Zentrum für Schwerionenforschung GmbH, D-64291 Darmstadt, Germany*
[4]*Key Laboratory of Nuclear Data, China Institute of Atomic Energy, Beijing 102413, China*
[5]*School of Physics and State Key Laboratory of Nuclear Physics and Technology, Peking University, Beijing 100871, China*
[6]*School of Physics, Engineering and Technology, University of York, York YO10 5DD, United Kingdom*
[7]*Advanced Science Research Center (ASRC), Japan Atomic Energy Agency, Tokai-mura, Japan*
[8]*Department of Nuclear Physics and Biophysics, Comenius University in Bratislava, 84248 Bratislava, Slovakia*
[9]*School of Space Science and Physics, Shandong University, Weihai 264209, China*
[10]*The Key Laboratory of Beam Technology of Ministry of Education, College of Nuclear Science and Technology, Beijing Normal University, Beijing 100875, China*
[11]*Institute of Radiation Technology, Beijing Academy of Science and Technology, Beijing 100875, China*

(Received 12 March 2024; revised 30 May 2024; accepted 3 July 2024; published 25 July 2024)

The near-symmetric complete fusion reaction $^{78}\mathrm{Kr} + {}^{107}\mathrm{Ag} \rightarrow {}^{185}\mathrm{Bi}^{*}$ was studied at the gas-filled recoil separator SHANS with an attempt to synthesize the extremely neutron-deficient proton-unbound ^{182,183}Bi isotopes. No decay events which could be attributed to them were observed. The two- and three-particle evaporation residues ^{180,179}Hg (αp, αpn) and ^{183,182}Pb (pn, $p2n$) were identified. Their production cross sections have been measured at two bombarding energies. Based on the yields of ^{182,183}Pb in the present work and the systematics of the ratios between the cross sections of $p(x\text{-}1)n$ and xn evaporation channels for the most neutron-deficient odd-Z nuclei above lead, the upper limits for the half-lives of ^{182,183}Bi were estimated to be less than 0.3 μs.

DOI: 10.1103/PhysRevC.110.014326

I. INTRODUCTION

The neutron-deficient nuclei around the proton shell closure at $Z = 82$ and the neutron midshell at $N = 104$ exhibit a variety of interesting nuclear structure and decay phenomena, including shape coexistence [1–6], α decay, proton radioactivity [7–11], and β-delayed fission [12,13]. One of the methods to reach this region of nuclei is complete fusion reaction with heavy ions. However, the production cross sections of the most neutron-deficient nuclei known in this region decrease to nanobarn levels or even lower, due to the rapidly decreasing fission barriers of the compound nuclei and the strong competition from charged-particle evaporation channels. The experimental excitation functions of evaporation residues (ERs) are crucial for determining the optimal beam energies and estimating the cross sections for new neutron-deficient nuclei.

So far, the lightest known bismuth isotope is ^{184}Bi, synthesized in the complete fusion ^{93}Nb(^{94}Mo, $3n$) reaction, about two decades ago at SHIP [14]. In this experiment, two α-decaying states with half-lives of 13(2) ms and 6.6(15) ms were observed [14]. Because of their yet unknown relative ordering, they were denoted as two isomeric states (^{184m1,m2}Bi). The same situation happens in ^{186}Bi, where two α-decaying states (^{186m1,m2}Bi) with half-lives of 9.8(4) ms and 14.8(8) ms were identified [14]. The quite similar half-lives for respective states in both isotopes could be understood in terms of the similar energies of their strongest unhindered α decays (7.1–7.3 MeV) feeding the excited intruder states in their daughters ^{180,182}Tl, as shown in Fig. 7(a) of Ref. [14]. Assuming such predominant feeding to yet unknown excited state(s) in ^{178}Tl also applies to the lighter odd-odd ^{182}Bi isotope, a half-life of the order of milliseconds could be expected for its α-decaying state(s), due to the reduced α-decay energy. On the other hand, if this mechanism is not present anymore, the α decays to the ground state (g.s.) in ^{178}Tl are expected to have much higher energy (see systematics in Fig. 7(a) of Ref. [14]), which will result in a much shorter half-life. Furthermore, proton emission cannot be ruled out for ^{182}Bi, as ^{185}Bi is known with a dominant proton-decay branch [7–10].

The relatively long half-lives for ^{184,186}Bi are in strong contrast to the half-life of $2.8^{+2.3}_{-1.0}$ μs for the $1/2^{+}$ g.s. in ^{185}Bi, which was recently identified at Argonne National

*Contact author: liuzhong@impcas.ac.cn
†Contact author: zhli@pku.edu.cn
‡Contact author: andrei.andreyev@york.ac.uk

TABLE I. Experimental cross sections for the ERs in the ^{78}Kr + ^{107}Ag reaction measured in the present work. The beam energies in the middle of the targets and the average currents are listed in column 1 and 2, respectively.

			Cross section (μb)[a]			
Energy	Beam current	Time	^{180}Hg(αp)	^{179}Hg(αpn)	^{182}Pb(pn)	^{183}Pb($p2n$)
338 MeV	130 pnA	30 h	0.67(8)	0.19(9)	0.004(1)	0.021(4)
342 MeV	100 pnA	109 h	1.05(7)	0.5(2)	0.009(1)	0.025(4)

[a]The errors of cross sections arising from the uncertainties of the beam intensities, which were estimated to be 50% and are not listed in the table.

Laboratory [10]. This also redefined the previously known 58(2)-μs decay as the excited isomeric state, instead of its earlier assignment as the $1/2^+$ g.s. in ^{185}Bi [7–9]. Based on a well-established linear systematics of the proton- and α-decay energies (Q_p and Q_α) from the $1/2^+$ isomer or g.s. in the heavier odd-A Bi isotopes ($^{185-191}$Bi) [15–17], the Q_p and Q_α of the possible $1/2^+$ g.s. in ^{183}Bi were extrapolated to be around 2.1 MeV and 8.7 MeV, respectively. The corresponding short partial half-lives of ≈ 24 ns and ≈ 1 μs were estimated by using the universal decay law (UDL) deduced in Refs. [18–21], which will be extremely challenging for the recoil separator. However, the possible existence of the longer-lived isomer similar to that in ^{185}Bi cannot be ruled out.

In the present work, the ^{78}Kr + ^{107}Ag → ^{185}Bi* reaction was studied at the gas filled separator SHANS to produce new isotopes ^{182,183}Bi via $3n$ and $2n$ evaporation channels, respectively. However, no events associated with them were observed and possible limits for their half-lives are discussed. The cross sections of the ERs produced in pxn and αpxn evaporation channels were measured at two bombarding energies.

II. EXPERIMENT

The experiments were carried out at the gas-filled recoil separator SHANS (Spectrometer for Heavy Atoms and Nuclear Structure) [22]. The ^{78}Kr ions with energies of 349 and 353 MeV were provided by the Sector-Focusing Cyclotron (SFC) of the Heavy Ion Research Facility in Lanzhou (HIRFL), China. The beam intensity was measured by a Faraday cup installed at the exit of the SFC. The self-supporting ^{107}Ag targets (∼97.8% enrichment with about 2.2% ^{109}Ag) had an average thickness of ∼900 μg/cm^2. Energy losses in the targets were calculated using the SRIM code [23]. The beam energies in the middle of the targets, the average beam intensities, and the total beam-on-target time corresponding to these two beam energies are summarized in Table I.

The ERs were separated from the primary beam by SHANS filled with around 0.6-mbar helium gas. After separation, the ERs passed through two multiwire proportional counters (MWPCs) and then they were implanted into a double-sided silicon strip detector (DSSD) with 48×128 strips and a thickness of ∼300 μm, covering 48×128 mm^2. The energy calibration of the DSSD was performed with the known α-decay lines from ^{166,167}Os, ^{162,163}W, ^{158}Hf, and ^{167}Ir, produced in a reaction of ^{78}Kr + ^{92}Mo. The coincidence between signals from the MWPCs and the DSSD enabled implantations of ions to be distinguished from decays. The data were recorded using a general-purpose digital data acquisition system (GDDAQ) [24] and analyzed using the CERN ROOT framework [25]. The 16-μs waveforms from the preamplifiers of the DSSD were independently recorded with a sampling rate of 250 MHz. The pile-up signals with time separation down to 100 ns can be identified by combining visual check and effective pulse shape analysis algorithm [26,27].

In the present experiment, the use of heavy projectile ^{78}Kr induced a very strong flux of light particles like energetic protons or helium nuclei at the focal plane of SHANS. Therefore, three 4-strip silicon detectors, installed side by side behind the DSSD were used to veto these particles punching through the DSSD. However, about 7-mm wide dead regions between the adjacent veto detectors and the low detection efficiencies of MWPCs for energetic light particles still produced a strong light-particle background in the charged-particle decay spectroscopy. These energetic light particles, especially those punching through the DSSD, have higher ranges in DSSD than those of decays of ERs, causing longer rise-time in the DSSD preamplifier signals. A method developed to distinguish these energetic light particles from the α/p particles emitted in radioactive decays and suppress them will be described elsewhere [28].

III. RESULTS

Parts of the α-decay spectra registered in the DSSD, for the events measured following the implantation of the ERs within 5 s and 500 ms in the same pixel, are shown in Fig. 1(a) and (b), respectively. Due to the relatively long search interval [Δt(ER-α_m) < 5 s] applied, only the decays from isotopes with strongest evaporation channels can be seen in Fig. 1(a). The decays from weakly produced isotopes with short half-lives are present in Fig. 1(b), where the search interval is reduced down to 500 ms. The α_m-α_d (α_m and α_d refer to the mother and daughter α decays, respectively) position-time correlation spectrum from ER-α_m-α_d analysis is presented in Fig. 1(c). The respective time windows were set as Δt(ER-α_m) < 30 s and Δt(α_m-α_d) < 60 s.

Based on the correlations between the α_m and α_d decays shown in Fig. 1(c), the 5852-, 6120-, 6283-, 6693-, and 6901-keV α peaks shown in Fig. 1(a) and/or (b) are assigned to the α decays of ^{182,180,179}Hg and ^{183m,182}Pb, respectively. Due to the admixture of the 5848(5)-keV α decay of the g.s. in ^{179}Au [17,29], the energy of the 5852(8)-keV α peak in Fig. 1(a) is slightly lower than the evaluated α-decay energy [5867(5) keV] of ^{182}Hg g.s. in Refs. [17,30]. The α_m-α_d correlations of the ^{179}Au-^{175}Ir-^{171}Re chain cannot be distinguished

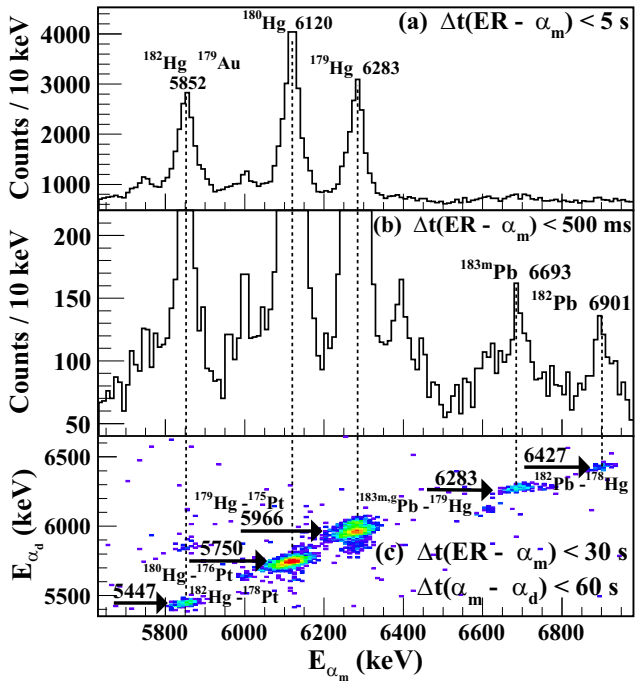

FIG. 1. (a) A part of the energy spectrum for the α particles recorded within 5 s after the ERs implantation in the ^{78}Kr + ^{107}Ag reaction. (b) The same spectrum as in (a), but with a search time of 500 ms. The α-decay peaks are labeled with their energy in keV and the isotopes they belong to. (c) Two-dimensional E_{α_m}-E_{α_d} plot for Δt(ER-α_m) < 30 s and $\Delta t(\alpha_m$-$\alpha_d)$ < 60 s.

from the random-coincidence background in Fig. 1(c), because of the very low branching ratio (0.85(28)% [17,31]) of the α decay from the daughter ^{175}Ir nucleus. Therefore, the α-decay properties of ^{182}Hg were deduced based on the α_m(^{182}Hg)-α_d(^{178}Pt) correlation analysis. Due to the limited statistics of two α-decay branches from the g.s. in ^{183}Pb, its half-life extraction was also based on the α_m(^{183g}Pb)-α_d(^{179}Hg) correlation analysis.

The α-decay energies and the half-lives of some ERs and their daughter isotopes identified in this experiment are summarized in Table II. A comparison with their evaluated values from Ref. [17] indicates good agreement for most of them.

A. Search for proton decays of ^{182,183}Bi

In order to identify the possible proton decays of ^{182,183}Bi, a search for spatial and temporal correlated ER-p-α_d events was carried out with the time interval of Δt(ER-p) < 30 ms and $\Delta t(p$-$\alpha_d)$ < 300 ms, covering over five times the half-lives (45(20) ms and 59(6) ms [17,36], respectively) of daughters ^{181,182}Pb. The corresponding two-dimensional energy plot is shown in Fig. 2(a), where the candidates for ^{182,183}Bi proton decays including the escaped events correlated with the full-energy 7004(7)-keV and 6911(6)-keV α decay of their daughters [17] are expected to appear in the transparent blue and red boxes, respectively. However, no such events were observed.

TABLE II. The α-decay properties of the ERs and their daughter isotopes extracted in the present experiment compared to the evaluated data [17]. The numbers of the ERs registered in the DSSD for g.s. or isomers (N_{ER}) were determined with Eq. (1).

Nuclide	E_α (keV) Exp.	E_α (keV) Lit. [17]	$T_{1/2}$ (s) Exp.	$T_{1/2}$ (s) Lit. [17]	N_{ER}
^{182}Hg	5857(7)	5867(5)	10(1)	10.83(6)	–
^{178}Pt	5447(8)	5446(3)	20(2)	21.1(6)	–
^{180}Hg	6120(6)	6119(4)	2.53(4)	2.58(1)	$64(2)\times10^3$
^{176}Pt	5750(6)	5753(3)	6.55(9)	6.3(4)	–
^{179}Hg	6283(6)	6285(3)	1.10(2)	1.05(3)	$29(13)\times10^3$
^{175}Pt	5966(6)	5948(4)[a]	2.35(5)	2.43(4)	–
^{183m}Pb	6693(7)	6704(6)	0.489(63)	0.415(20)	1028(79)
^{183g}Pb	6765(10)	6777(6)	0.537(94)	0.535(30)	325(184)[b]
	6562(10)	6576(6)			
^{182}Pb	6901(8)	6911(6)	0.062(8)	0.059(6)	530(42)
^{178}Hg	6427(8)	6430(6)	0.248(24)	0.266(25)	–

[a]A value of 5963(5) keV was measured in Ref. [30], is in agreement with our value and the results in other experiments [32–35].
[b]Extracted based on the α_m(^{183g}Pb)-α_d(^{179}Hg) correlation analysis and corrected with the α-decay branching ratio of the daughter ^{179}Hg.

B. Search for α decays of ^{182,183}Bi

Due to the longer half-lives (254^{+11}_{-9} ms and 230(40) ms [17,37,38], respectively) of the g.s. in the daughter ^{178,179}Tl, possibly fed by the α decays of ^{182,183}Bi, the correlation search time of $\Delta t(\alpha_m$-$\alpha_d)$ was extended to 2 s, about eight times their half-lives. The correlated events are shown in Fig. 2(b). The regions for the candidate events of ^{182,183}Bi are also shown with transparent blue and red boxes, as in Fig. 2(a). Three expected transitions corresponding to the α decays of ^{178}Tl [6595(10) keV (24(5)%), 6693(10) keV(70(4)%), and 6862(10)keV (6(3)%) [17,39]] are shown with three blue boxes in Fig. 2(b). Since escaped α particles deposit energies above ∼1 MeV [see the energy distributions for the escaped α decays of ^{182}Pb and ^{179m}Tl in Figs. 2(a) and 2(b)], four points in the green ellipse cannot be attributed to the correlated events of ^{182,183}Bi. The half-life and decay energy of the second-generation decay in this cluster were deduced to be $0.5^{+0.5}_{-0.2}$ s and 6563(19) keV, respectively. They are consistent with the decay of ^{179g}Tl($T_{1/2}$ = 0.23(4) s, E_α = 6567(8) keV [17,38]) within statistics. The half-life of these low-energy events were obtained to be $1.3^{+1.3}_{-0.4}$ ms, which is in good agreement with the evaluated value (1.5(3) ms [17]) of the isomer in ^{179}Tl. These events are thus interpreted as conversion electrons from internal transition of ^{179m}Tl and provide the first evidence for this decay, which was anticipated in Ref. [40]. This decay path will be discussed in a separate publication.

The chain in the red ellipse (E_{α_m} = 1603 keV, T_m = 83 μs, E_{α_d} = 6604 keV, and T_d = 606 ms) was followed by a grand-daughter α decay with E_{α_g} = 6092 keV and T_g = 1 s. The properties of all three generations in this chain match with the known full-energy p/α-decay data for ^{185}Bi (E_p = 1598(16) keV, $T^m_{1/2}$ = 58(2) μs [10,17]), ^{184}Pb(E_α = 6627(6) keV, $T_{1/2}$ = 490(25) ms [17]), and ^{180}Hg (E_α = 6119(4) keV,

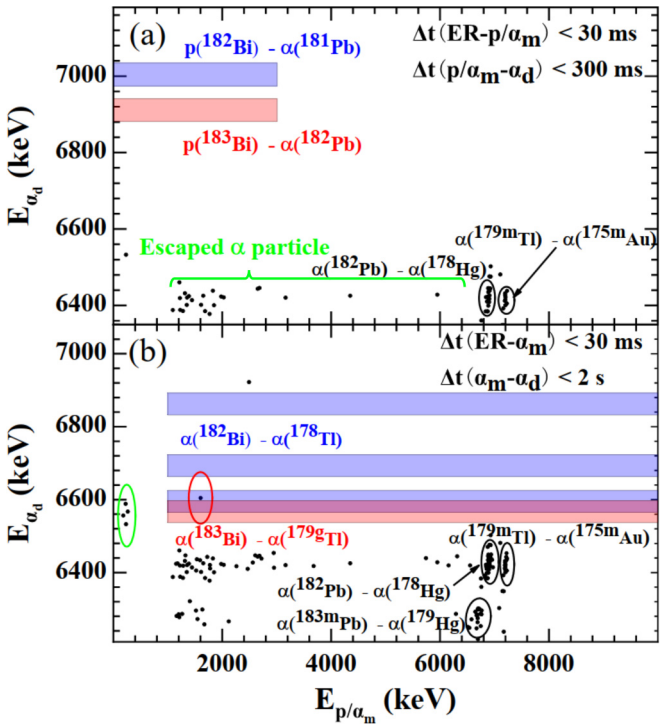

FIG. 2. (a) Two-dimensional E_{p/α_m}-E_{α_d} plot for Δt(ER-α_m) < 30 ms and $\Delta t(\alpha_m$-$\alpha_d)$ < 300 ms in the ^{78}Kr + ^{107}Ag reaction. (b) The same as (a) but with the time interval of $\Delta t(\alpha_m$-$\alpha_d)$ < 2 s. The regions for the candidate p/α_m (including the escaped events)-α_d decay chains of ^{182,183}Bi are marked with transparent blue and red boxes, respectively. The events in the green ellipse in (b) could be associated with the CE of internal transition in the cascade depopulating the $11/2^-$ isomer of ^{179}Tl (see text for details). The event in red ellipses can be interpreted as a proton decay of ^{185}Bi (see text for details).

$T_{1/2} = 2.58(1)$ s [17,41,42]) within statistics. Therefore, this chain most likely originates from ^{185}Bi, which was produced in the ^{109}Ag(^{78}Kr, $2n$) reaction on the small admixture of ^{109}Ag in the target. The probability of a random correlation for this event is estimated to be less than 10^{-6} [43].

An event with $E_m = 2.5$ MeV and $E_d = 6.9$ MeV was observed in Fig. 2(b), which could be a candidate of the correlation for $p_m(^{183}\text{Bi})$-$\alpha_d(^{182}\text{Pb})$. However, their lifetimes were measured to be $T_m = 5.8$ ms and $T_d = 664$ ms, which are beyond ten times the expected proton-decay half-life of ^{183}Bi (of the order of μs) and evaluated value for ^{182}Pb (59(6) ms [17]), respectively. Therefore, this correlation is unlikely to be associated with $p_m(^{183}\text{Bi})$-$\alpha_d(^{182}\text{Pb})$ correlated event, and could be considered as random correlation.

We note that the g.s. in the daughter nuclei ^{178,179}Tl have about 40% β^+/electron capture (EC) branching ratios [17,44,45]. Therefore, the respective correlations with the full-energy α decays from the grand-daughters ^{178,179}Hg have been searched for. No candidate of α_m-β^+-α_g (α_g refers to the grand-daughter ^{178,179}Hg α decay) correlation was found either. The low energy charged particles (Auger or conversion electrons) accompanying the EC of ^{178,179}Tl are difficult to be observed in the DSSD, thus α_g from ^{178,179}Hg will be directly correlated with α_m from ^{182,183}Bi. Thanks to the shorter half-life of ^{183}Bi expected from the corresponding systematics of the heavier odd-A Bi isotopes, a reduced time window of Δt(ER-α_m) < 1 ms was used to search for $\alpha_m(^{183}\text{Bi})$-$\alpha_g(^{179}\text{Hg})$ correlation, but none was observed. However, it would not be possible to distinguish the α_m (^{182}Bi)-α_g (^{178}Hg) correlations from α_m (^{182}Pb and ^{179m}Tl)-α_d (^{178}Hg and ^{175m}Au) correlations.

We also considered the possibility of very short (μs and sub-μs) half-lives for ^{182,183}Bi, as, e.g., the half-life of the g.s. in ^{185}Bi is only $2.8^{+2.3}_{-1.0}$ μs [10]. The signals of the p/α decay could pile up on that of the ERs, resulting in their absence in Fig. 2. The traces of the ERs followed by the full-energy α decays of the daughter nuclei (^{182,181}Pb, ^{178,179}Tl) mentioned above have been checked by visual check and using effective pulse shape analysis algorithm [26,27], but no pile-up signals were identified.

To conclude, no proton or α decay of ^{182,183}Bi was identified in the present study.

C. Cross-section measurements of the ERs

The numbers of ERs registered in the DSSD for the g.s. or isomers ($N_{ER}^{g,m}$) were extracted by using the following expression:

$$N_{ER}^{g,m} = \frac{N_\alpha^{g,m}}{b_\alpha^{g,m}\epsilon_\alpha}, \quad (1)$$

where $N_\alpha^{g,m}$ is the numbers of the full-energy α decays and $b_\alpha^{g,m}$ is the corresponding branching ratios [17]; $\epsilon_\alpha = 60(2)\%$ is the efficiency of the DSSD for detection of the full-energy events. The results are presented in the last column of Table II. For ^{178,179}Hg and ^{182}Pb, only the g.s. are known to disintegrate via a charged particle decay, so the corresponding values can be taken as their total yields. Based on the $N_{^{183}Pb}^{m,g}$ listed in Table II, a total of 1300 ERs of ^{183}Pb were registered in the DSSD. Assuming SHANS transmission efficiency of 14% [22], the production cross sections for the ERs in the ^{78}Kr + ^{107}Ag complete fusion reaction have been deduced, and are listed in Table I.

IV. DISCUSSION

The experimental production cross sections of Bi, At, and Fr isotopes in neutron-evaporation channels, measured at different gas-filled or vacuum separators, around the corresponding optimum beam energies are shown in blue in the chart in Fig. 3. To avoid the possible influence of proton pairing, especially on the fission barriers of the compound nuclei, the even-Z isotopes are excluded. It should be noted that the cross section of ^{185}Bi shown in bracket in Fig. 3 was mostly probably underestimated due to short half-lives of its g.s. ($2.8^{+2.3}_{-1.0}$ μs [10]) in comparison to the long dead time (∼15 μs) of the analog electronics system used in Ref. [46].

Based on the experimental cross sections of these ERs produced in the xn and their isobars in the $p(x-1)n$ channels [46–54], their ratios around their maxima of the excitation functions were collected and are shown in red in the chart in Fig. 3. For the odd-Z isotopes (Bi, At, and Fr), the ratios $\sigma(pn)/\sigma(2n)$ and $\sigma(p2n)/\sigma(3n)$ around the

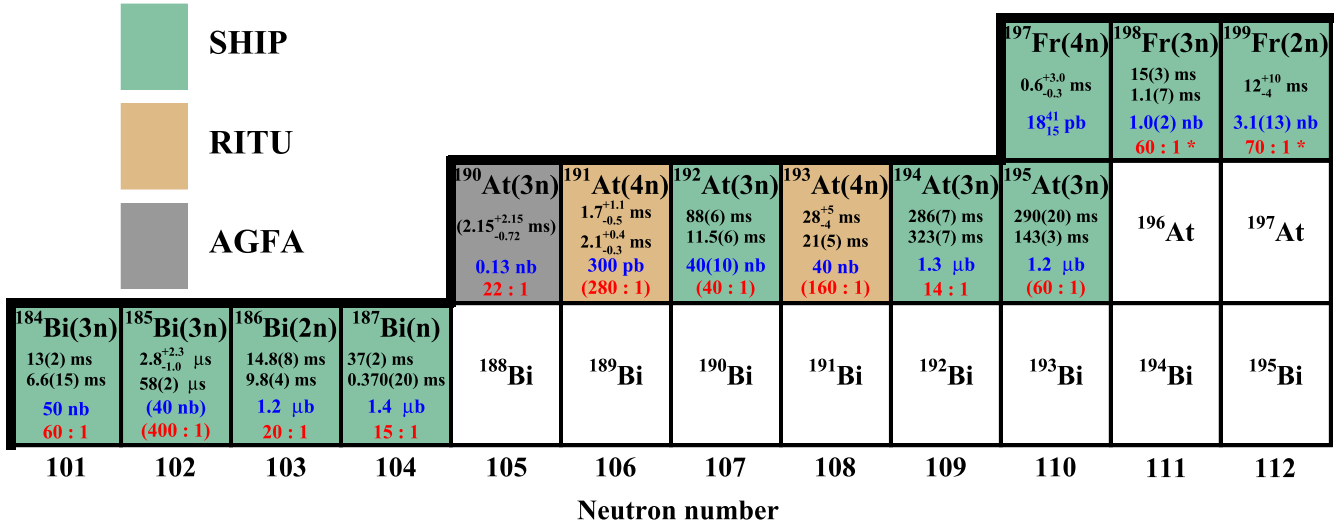

FIG. 3. Excerpt of the nuclear chart for the odd-Z neutron-deficient nuclei above Pb. Their production cross sections in the neutron-evaporation channels (the specific channels are shown behind the name of the isotopes in the brackets) of the complete fusion reactions around the optimum beam energies are shown with blue labels [46–54]. Colored squares represent the cross sections were measured at SHIP, RITU, and AGFA, respectively [46–54]. The ratios of $\sigma(p(x-1)n)/\sigma(xn)$ in the corresponding reactions are shown with red labels. The ratios for ^{198,199}Fr (labeled with stars) were deduced based on the experimental cross sections from Ref. [54]. The ratios estimated based on the α-decay spectra reported in the literature [48,50,52] or related to ^{185}Bi [46] are shown in the brackets. The evaluated or experimental half-lives of their g.s. and isomers de-exciting dominantly by the α/p decays are labeled in black. The half-life of ^{190}At which corresponds to one of two possible scenarios presented in Ref. [47] is shown in the bracket. The thick black lines indicate the limits of known isotopes.

optimum beam energies are expected to be ∼50(30) and ∼40(25), respectively. Higher ratios over ∼150 were deduced for $\sigma(p3n)/\sigma(4n)$. The xn and $p(x-1)n$ excitation functions covering the wide energy ranges in the complete fusion reactions leading to the neutron-deficient ^{187,188}Bi* compound nuclei have been measured at SHIP [46]. As excitation energy changes, no significant variation in $\sigma(p(x-1)n)/\sigma(xn)$ ratios was observed in either HIVAP calculations or experimental data (see Figs. 6 and 7 in Ref. [46]). Therefore, the results mentioned above could be approximately applicable at the two beam energies in the present experiment.

Based on the aforementioned $\sigma(pn)/\sigma(2n)$ ratio of ∼50(30) and total yield of ^{183}Pb (∼1300 events), about 26 ^{183}Bi ERs are expected to be detected in the DSSD in the present work. The α-decay branching ratios of its p- and α-decay daughters (^{182}Pb and ^{179}Tl) are 98% [17,44] and 60% [45], respectively. Combined with the 60% efficiency of the DSSD for full-energy α decays, at least $26\times60\%\times60\% = 9p/\alpha$ decays of ^{183}Bi followed by the full-energy α decays of their daughter nuclei (^{182}Pb/^{179}Tl) are expected to be measured in the present experiment. However, no candidates for such p_m/α_m-α_d correlation pairs were observed, indicating that all of the ^{183}Bi nuclei produced in the present experiment have decayed before reaching the DSSD. The time of flight of the ERs through SHANS is about 600 ns. Assuming the observation limit of one count of this decay, an upper limit of ∼0.19(6) μs for the half-life of ^{183}Bi can be deduced, which is in agreement with the prediction of the UDL (see the details in Sec. I). Similarly, an upper limit of ∼0.26(12) μs for the half-life of ^{182}Bi was estimated.

It should be noted that another reason for nonobservation of the correlated events associated with ^{182,183}Bi, besides the short-lifetime, is their low production cross sections in the present experiment. For example, assuming sufficiently long half-lives to survive the flight through SHANS (e.g., >1 μs), the corresponding cross sections would be about 50 pb and the ratios of $\sigma(pn)/\sigma(2n)$ and $\sigma(p2n)/\sigma(3n)$ in the $^{78}\mathrm{Kr}+{}^{107}\mathrm{Ag}\rightarrow{}^{185}\mathrm{Bi}^*$ reaction would be ∼500 and ∼200, respectively. Based on the systematics of $\sigma(pn)/\sigma(2n)$ and $\sigma(p2n)/\sigma(3n)$ ratios in heavier Bi and other odd-Z isotopes above lead (see Fig. 3), the first case, i.e., short half-life, is more likely than this scenario.

A. The decays and structure of ^{183}Bi

The $1/2^+$ intruder state originating from a mixed prolate-oblate configuration based on the $\pi 3s_{1/2}$ orbital, with a relatively small deformation of $\beta_2 \sim 0.15$ was identified as the $2.8^{+2.3}_{-1.0}$-μs g.s. in ^{185}Bi [10]. Its unhindered proton and α decays to the respective g.s. of ^{184}Pb and ^{181}Tl, rather than to their excited states [see Fig. 4(b)], can explain the short half-life of the g.s. in ^{185}Bi. As suggested by the calculated excitation energies of some selected configuration shown in Fig. 8 of Ref. [9], several deformed $1/2^+$ states have strong downward excitation energy trend, culminating in the observed $1/2^+$ g.s. in ^{185}Bi. By analogy with ^{185}Bi, the unhindered fast decay (most probably the pure proton emission) from the $1/2^+$ intruder g.s. can be expected in ^{183}Bi. Due to the increased Q_p and Q_α values (see Sec. I), the half-life should be even shorted than in ^{185}Bi, which is in

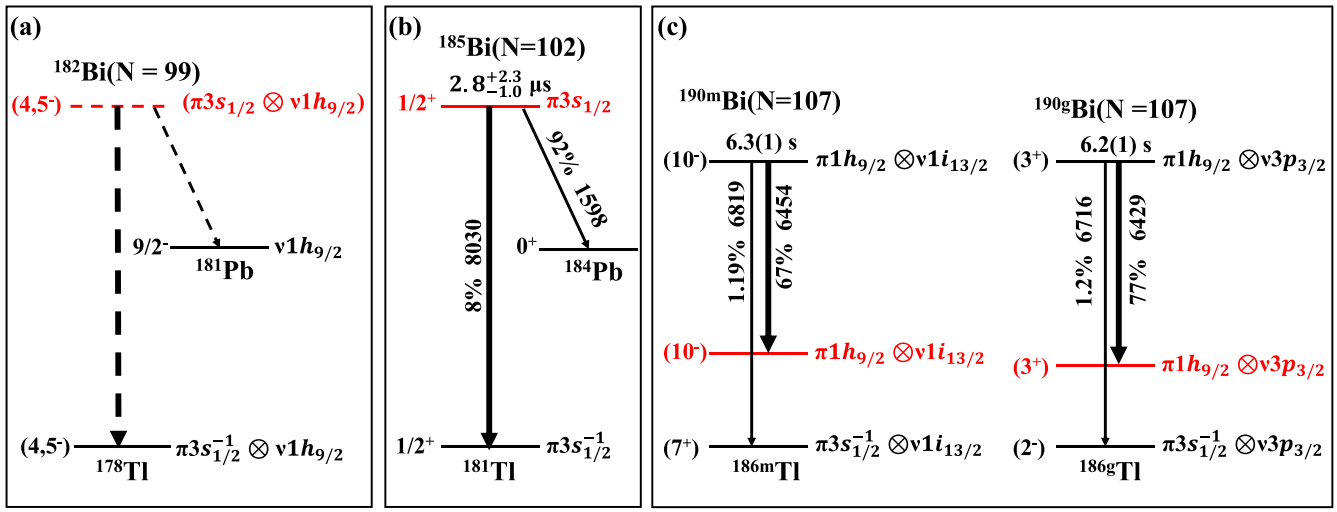

FIG. 4. (a) The tentative decay scheme for ^{182}Bi. The partial decay schemes of ^{185,190m,g}Bi [(b) and (c)] [10,17,55]. The hindered highest-energy and unhindered (strongest) α decays are shown by thin and thick lines, respectively. The proton emissions are also shown in thin lines. The tentative spins, parities, and configurations assignments except of ^{182}Bi are taken from Refs. [10,39,55,56]. The intruder states are shown in red.

agreement with our interpretation that the non-observation of ^{183}Bi in our study is caused by a short half-life.

B. Similarities in the α decays of odd-odd $^{184-196}$Bi isotopes

In the heavier odd-odd $^{190-196}$Bi isotopes the spins and parities of the α-decaying g.s. and isomers were tentatively assigned as (3^+) and (10^-), respectively [17,55,57,58]. The example of ^{190m,g}Bi is shown in Fig. 4(c). Their α decays dominantly feed the excited intruder states [shown in red in Fig. 4(c)] with the same spins, parities, and configurations, instead of the g.s. or excited isomer in the respective daughter Tl isotopes [17,55,57,58].

A similar pattern with (10^-) and (3^+) α-decaying states and dominant feeding to the excited intruder states was initially proposed for ^{188m,g}Bi (see Fig. 4 of Ref. [55]) [17,55,58–60]. However, the recent laser-spectroscopy study at the ISOLDE facility (CERN) reinterpreted the low-spin state as a strongly deformed $1^{(+)}$ state whose structure is determined by the blocked configuration $\pi 1/2[530] \otimes \nu 1/2[521]$ [6].

Similar to odd-odd $^{188-196}$Bi isotopes, two observed α-decaying states in ^{184,186}Bi isotopes decay to the excited states rather than the g.s. in the daughters ^{180,182}Tl [14,61]. The expected increase in energy of the excited intruder states in the daughter Tl isotopes was proposed as the explanation for the similar Q_α values for the main decays of the parent Bi isotopes, resulting in their approximate half-lives of about 10 ms (see the discussion of Fig. 7(a) in Ref. [14]). As we will suggest below, this mechanism breaks in ^{182}Bi.

C. The decays and structure of ^{182}Bi

As deduced in our study, ^{182}Bi possesses a very short half-life, indicating unhindered proton and/or α decays with a large Q_p and/or Q_α values [see Fig. 4(a)] In the α decay case, this implies that the configuration of ^{182}Bi, shown in red in Fig. 4(a), should be similar to that of the daughter ^{178}Tl ($[\pi 3s^{-1}_{1/2} \otimes \nu 1h_{9/2}]_{4,5^-}$ [39]). This inference is quite natural since at $N \leqslant 100$ neutron orbital $\nu 1h_{9/2}$ comes into play, due to the complete depletion of $\nu 3p_{3/2}$ and $\nu 1i_{13/2}$ orbitals [39].

The g.s. with the spin-parity assignment of $I^\pi = 9/2^-$ in ^{181}Pb was suggested to be based on the spherical $\nu 1h_{9/2}$ orbital [56], which would be the same as the valence neutron in ^{182}Bi [see Fig. 4(a)]. Therefore, the proton decay from the g.s. in ^{182}Bi to this state [see the thin dashed line in Fig. 4(a)] could be unhindered, which would also result in a very short half-life, due to high expected Q_p value.

V. SUMMARY

An attempt to synthesize the very neutron-deficient ^{182,183}Bi isotopes using the ^{78}Kr + ^{107}Ag complete fusion reaction was carried out at the gas-filled separator SHANS. No respective events were observed. The production cross sections of the two- and three-particle ERs ^{182,183}Pb and ^{179,180}Hg were measured at two incident energies. Based on the systematics of the cross-section ratios between the $p(x\text{-}1)n$ and xn channels in complete fusion reaction with neutron-deficient compound nuclei above Pb, upper limits for the half-lives of ^{182}Bi and ^{183}Bi were deduced to be 0.26(12) μs and 0.19(6) μs, respectively. Therefore, this is extremely challenging for the available experimental techniques.

ACKNOWLEDGMENTS

The authors thank the HIRFL staff as well as the ion source crew for delivering the stable ^{78}Kr beam. This work has been supported by the National Natural Science Foundation of China (Grants No. 12135004, No. 11961141004, and No. U2167201), the Strategic Priority

Research Program of Chinese Academy of Sciences (Grant No. XDB34000000), the National Key R&D Program of China (Contract No. 2018YFA0404402), Slovak Research and Development Agency (Contract No. APVV-22-0282), and Slovak Grant Agency VEGA (Project No. 1/0651/21). A.N.A. is grateful for financial support from the STFC and the Chinese Academy of Sciences President's International Fellowship Initiative (Grant No. 2020VMA0017).

[1] K. Heyde and J. L. Wood, Rev. Mod. Phys. **83**, 1467 (2011).
[2] J. L. Wood and K. Heyde, J. Phys. G: Nucl. Part. Phys. **43**, 020402 (2016).
[3] A. N. Andreyev, M. Huyse, P. Van Duppen, L. Weissman, D. Ackermann, J. Gerl, F. P. Hessberger, S. Hofmann, A. Kleinböhl, G. Münzenberg, S. Reshitko, C. Schlegel, H. Schaffner, P. Cagarda, M. Matos, S. Saro, A. Keenan, C. Moore, C. D. O'Leary, R. D. Page *et al.*, Nature (London) **405**, 430 (2000).
[4] B. A. Marsh, T. Day Goodacre, S. Sels, Y. Tsunoda, B. Andel, A. N. Andreyev, N. A. Althubiti, D. Atanasov, A. E. Barzakh, J. Billowes, K. Blaum, T. E. Cocolios, J. G. Cubiss, J. Dobaczewski, G. J. Farooq-Smith, D. V. Fedorov, V. N. Fedosseev, K. T. Flanagan, L. P. Gaffney, L. Ghys *et al.*, Nat. Phys. **14**, 1163 (2018).
[5] S. Sels, T. Day Goodacre, B. A. Marsh, A. Pastore, W. Ryssens, Y. Tsunoda, N. Althubiti, B. Andel, A. N. Andreyev, D. Atanasov, A. E. Barzakh, M. Bender, J. Billowes, K. Blaum, T. E. Cocolios, J. G. Cubiss, J. Dobaczewski, G. J. Farooq-Smith, D. V. Fedorov, V. N. Fedosseev *et al.*, Phys. Rev. C **99**, 044306 (2019).
[6] A. Barzakh, A. N. Andreyev, C. Raison, J. G. Cubiss, P. Van Duppen, S. Péru, S. Hilaire, S. Goriely, B. Andel, S. Antalic, M. Al Monthery, J. C. Berengut, J. Bieroń, M. L. Bissell, A. Borschevsky, K. Chrysalidis, T. E. Cocolios, T. Day Goodacre, J.-P. Dognon, M. Elantkowska *et al.*, Phys. Rev. Lett. **127**, 192501 (2021).
[7] C. N. Davids, P. J. Woods, H. T. Penttilä, J. C. Batchelder, C. R. Bingham, D. J. Blumenthal, L. T. Brown, B. C. Busse, L. F. Conticchio, T. Davinson, D. J. Henderson, R. J. Irvine, D. Seweryniak, K. S. Toth, W. B. Walters, and B. E. Zimmerman, Phys. Rev. Lett. **76**, 592 (1996).
[8] G. L. Poli, C. N. Davids, P. J. Woods, D. Seweryniak, M. P. Carpenter, J. A. Cizewski, T. Davinson, A. Heinz, R. V. F. Janssens, C. J. Lister, J. J. Ressler, A. S. Sonzogni, J. Uusitalo, and W. B. Walters, Phys. Rev. C **63**, 044304 (2001).
[9] A. N. Andreyev, D. Ackermann, F. P. Heβberger, K. Heyde, S. Hofmann, M. Huyse, D. Karlgren, I. Kojouharov, B. Kindler, B. Lommel, G. Münzenberg, R. D. Page, K. Van de Vel, P. Van Duppen, W. B. Walters, and R. Wyss, Phys. Rev. C **69**, 054308 (2004).
[10] D. T. Doherty, A. N. Andreyev, D. Seweryniak, P. J. Woods, M. P. Carpenter, K. Auranen, A. D. Ayangeakaa, B. B. Back, S. Bottoni, L. Canete, J. G. Cubiss, J. Harker, T. Haylett, T. Huang, R. V. F. Janssens, D. G. Jenkins, F. G. Kondev, T. Lauritsen, C. Lederer-Woods, J. Li, C. Müller-Gatermann, D. Potterveld, W. Reviol, G. Savard, S. Stolze, and S. Zhu, Phys. Rev. Lett. **127**, 202501 (2021).
[11] H. Kettunen, T. Enqvist, T. Grahn, P. T. Greenlees, P. Jones, R. Julin, S. Juutinen, A. Keenan, P. Kuusiniemi, M. Leino, A.-P. Leppänen, P. Nieminen, J. Pakarinen, P. Rahkila, and J. Uusitalo, Phys. Rev. C **69**, 054323 (2004).
[12] A. N. Andreyev, S. Antalic, D. Ackermann, L. Bianco, S. Franchoo, S. Heinz, F. P. Heßberger, S. Hofmann, M. Huyse, Z. Kalaninová, I. Kojouharov, B. Kindler, B. Lommel, R. Mann, K. Nishio, R. D. Page, J. J. Ressler, B. Streicher, S. Saro, B. Sulignano, and P. Van Duppen, Phys. Rev. C **87**, 014317 (2013).
[13] A. N. Andreyev, M. Huyse, and P. Van Duppen, Rev. Mod. Phys. **85**, 1541 (2013).
[14] A. N. Andreyev, D. Ackermann, F. P. Heßberger, S. Hofmann, M. Huyse, I. Kojouharov, B. Kindler, B. Lommel, G. Münzenberg, R. D. Page, K. V. de Vel, P. V. Duppen, and K. Heyde, Eur. Phys. J. A **18**, 55 (2003).
[15] W. Q Zhang *et al.*, Phys. Rev. C (to be published).
[16] F. G. Kondev, M. Wang, W. J. Huang, S. Naimi, and G. Audi, Chin. Phys. C **45**, 030001 (2021).
[17] Evaluated Nuclear Structure Data File (ENSDF), https://www.nndc.bnl.gov/ensdf.
[18] C. Qi, D. S. Delion, R. J. Liotta, and R. Wyss, Phys. Rev. C **85**, 011303(R) (2012).
[19] C. Qi, F. R. Xu, R. J. Liotta, and R. Wyss, Phys. Rev. Lett. **103**, 072501 (2009).
[20] C. Qi, F. R. Xu, R. J. Liotta, R. Wyss, M. Y. Zhang, C. Asawatangtrakuldee, and D. Hu, Phys. Rev. C **80**, 044326 (2009).
[21] C. Qi, R. J. Liotta, and R. Wyss, J. Phys.: Conf. Ser. **381**, 012131 (2012).
[22] Z. Zhang, L. Ma, Z. Gan, M. Huang, T. Huang, G. Li, X. Wu, G. Jia, L. Yu, H. Yang, Z. Sun, X. Zhou, H. Xu, and W. Zhan, Nucl. Instrum. Methods Phys. Res. B **317**, 315 (2013).
[23] J. F. Ziegler, M. Ziegler, and J. Biersack, Nucl. Instrum. Methods Phys. Res. B **268**, 1818 (2010).
[24] H. Wu, Z. Li, H. Tan, H. Hua, J. Li, W. Hennig, W. Warburton, D. Luo, X. Wang, X. Li, S. Zhang, C. Xu, Z. Chen, C. Wu, Y. Jin, J. Lin, D. Jiang, and Y. Ye, Nucl. Instrum. Methods Phys. Res. A **975**, 164200 (2020).
[25] R. Brun and F. Rademakers, Nucl. Instrum. Methods Phys. Res. A **389**, 81 (1997).
[26] X. Wang, Z. Li, Z. Liu, J. Li, H. Hua, H. Lu, W. Zhang, T. Huang, M. Sun, J. Wang, X. Liu, B. Ding, Z. Gan, L. Ma, H. Yang, Z. Zhang, L. Yu, J. Jiang, K. Wang, Y. Wang *et al.*, Nucl. Instrum. Methods Phys. Res. A **971**, 164068 (2020).
[27] H. Y. Lu, Z. Liu, Z. H. Li, X. Wang, J. Li, H. Hua, H. Huang, W. Q. Zhang, Q. B. Zeng, X. H. Yu, T. H. Huang, M. D. Sun, J. G. Wang, X. Y. Liu, B. Ding, Z. G. Gan, L. Ma, H. B. Yang, Z. Y. Zhang, L. Yu *et al.*, Phys. Rev. C **108**, 014302 (2023).
[28] H. Y Wu *et al.* (unpublished).
[29] A. Siivola, Nucl. Phys. A **109**, 231 (1968).
[30] E. Hagberg, P. Hansen, P. Hornshøj, B. Jonson, S. Mattsson, and P. Tidemand-Petersson, Nucl. Phys. A **318**, 29 (1979).
[31] J. Keller, K.-H. Schmidt, F. Hessberger, G. Münzenberg, W. Reisdorf, H.-G. Clerc, and C.-C. Sahm, Nucl. Phys. A **452**, 173 (1986).
[32] A. Rytz, At. Data Nucl. Data Tables **47**, 205 (1991).
[33] H. Gauvin, R. Hahn, Y. Le Beyec, M. Lefort, and J. Livet, Nucl. Phys. A **208**, 360 (1973).
[34] A. Siivola, Nucl. Phys. **84**, 385 (1966).

[35] P. Hansen, H. Nielsen, K. Wilsky, M. Alpsten, M. Finger, A. Lindahl, R. Naumann, and O. Nielsen, Nucl. Phys. A **148**, 249 (1970).

[36] K. S. Toth, J. C. Batchelder, C. R. Bingham, L. F. Conticchio, W. B. Walters, C. N. Davids, D. J. Henderson, R. Herman, H. Penttilä, J. D. Richards, A. H. Wuosmaa, and B. E. Zimmerman, Phys. Rev. C **53**, 2513 (1996).

[37] M. W. Rowe, J. C. Batchelder, T. N. Ginter, K. E. Gregorich, F. Q. Guo, F. P. Hessberger, V. Ninov, J. Powell, K. S. Toth, X. J. Xu, and J. Cerny, Phys. Rev. C **65**, 054310 (2002).

[38] K. S. Toth, X.-J. Xu, C. R. Bingham, J. C. Batchelder, L. F. Conticchio, W. B. Walters, L. T. Brown, C. N. Davids, R. J. Irvine, D. Seweryniak, J. Wauters, and E. F. Zganjar, Phys. Rev. C **58**, 1310 (1998).

[39] V. Liberati, A. N. Andreyev, S. Antalic, A. Barzakh, T. E. Cocolios, J. Elseviers, D. Fedorov, V. N. Fedoseeev, M. Huyse, D. T. Joss, Z. Kalaninová, U. Köster, J. F. W. Lane, B. Marsh, D. Mengoni, P. Molkanov, K. Nishio, R. D. Page, N. Patronis, D. Pauwels *et al.*, Phys. Rev. C **88**, 044322 (2013).

[40] A. N. Andreyev, S. Antalic, D. Ackermann, T. E. Cocolios, V. F. Comas, J. Elseviers, S. Franchoo, S. Heinz, J. A. Heredia, F. P. Heßberger, S. Hofmann, M. Huyse, J. Khuyagbaatar, I. Kojouharov, B. Kindler, B. Lommel, R. Mann, R. D. Page, S. Rinta-Antila, P. J. Sapple *et al.*, J. Phys. G: Nucl. Part. Phys. **37**, 035102 (2010).

[41] F. G. Kondev, R. V. F. Janssens, M. P. Carpenter, K. A. Saleem, I. Ahmad, M. Alcorta, H. Amro, P. Bhattacharyya, L. T. Brown, J. Caggiano, C. N. Davids, S. M. Fischer, A. Heinz, B. Herskind, R. A. Kaye, T. L. Khoo, T. Lauritsen, C. J. Lister, W. C. Ma, R. Nouicer *et al.*, Phys. Rev. C **62**, 044305 (2000).

[42] S.-C. Wu and H. Niu, Nucl. Data Sheets **100**, 483 (2003).

[43] K. H. Schmidt, C. C. Sahm, K. Pielenz, and H. G. Clerc, Z. Phys. A **316**, 19 (1984).

[44] G. Audi, O. Bersillon, J. Blachot, and A. Wapstra, Nucl. Phys. A **729**, 3 (2003).

[45] A. N. Andreyev, V. Liberati, S. Antalic, D. Ackermann, A. Barzakh, N. Bree, T. E. Cocolios, J. Diriken, J. Elseviers, D. Fedorov, V. N. Fedosseev, D. Fink, S. Franchoo, S. Heinz, F. P. Heßberger, S. Hofmann, M. Huyse, O. Ivanov, J. Khuyagbaatar, B. Kindler *et al.*, Phys. Rev. C **87**, 054311 (2013).

[46] A. N. Andreyev, D. Ackermann, S. Antalic, I. G. Darby, S. Franchoo, F. P. Heßberger, S. Hofmann, M. Huyse, P. Kuusiniemi, B. Lommel, B. Kindler, R. Mann, G. Münzenberg, R. D. Page, S. Saro, B. Sulignano, B. Streicher, K. Vande Vel, P. V. Duppen, and D. R. Wiseman, Phys. Rev. C **72**, 014612 (2005).

[47] A. N. Andreyev, D. Seweryniak, B. Andel, S. Antalic, D. T. Doherty, A. Korichi, C. Barton, L. Canete, M. P. Carpenter, R. M. Clark, P. A. Copp, J. G. Cubiss, J. Heery, Y. Hrabar, H. Huang, T. Huang, V. Karayonchev, F. G. Kondev, T. Lauritsen, Z. Liu *et al.*, Phys. Rev. C **108**, 034303 (2023).

[48] H. Kettunen, T. Enqvist, T. Grahn, P. Greenlees, P. Jones, R. Julin, S. Juutinen, A. Keenan, P. Kuusiniemi, M. Leino, A.-P. Leppänen, P. Nieminen, J. Pakarinen, P. Rahkila, and J. Uusitalo, Eur. Phys. J. A **17**, 537 (2003).

[49] H. Kettunen, T. Enqvist, K. Eskola, T. Grahn, P. T. Greenlees, K. Helariutta, P. Jones, R. Julin, S. Juutinen, H. Kankaanpää, A. Keenan, H. Koivisto, P. Kuusiniemi, M. Leino, M. Leppänen, A. P.and Miukku, P. Nieminen, J. Pakarinen, P. Rahkila, and J. Uusitalo, Eur. Phys. J. A **25**, 181 (2005).

[50] A. N. Andreyev, S. Antalic, D. Ackermann, S. Franchoo, F. P. Heßberger, S. Hofmann, M. Huyse, I. Kojouharov, B. Kindler, P. Kuusiniemi, S. R. Lesher, B. Lommel, R. Mann, G. Münzenberg, K. Nishio, R. D. Page, J. J. Ressler, B. Streicher, S. Saro, B. Sulignano *et al.*, Phys. Rev. C **73**, 024317 (2006).

[51] A. N. Andreyev, S. Antalic, D. Ackermann, L. Bianco, S. Franchoo, S. Heinz, F. P. Heßberger, S. Hofmann, M. Huyse, I. Kojouharov, B. Kindler, B. Lommel, R. Mann, K. Nishio, R. D. Page, J. J. Ressler, P. Sapple, B. Streicher, i. c. v. Šáro, B. Sulignano *et al.*, Phys. Rev. C **79**, 064320 (2009).

[52] M. Nyman, S. Juutinen, I. Darby, S. Eeckhaudt, T. Grahn, P. T. Greenlees, U. Jakobsson, P. Jones, R. Julin, S. Ketelhut, H. Kettunen, M. Leino, P. Nieminen, P. Peura, P. Rahkila, J. Sarén, C. Scholey, J. Sorri, J. Uusitalo, and T. Enqvist, Phys. Rev. C **88**, 054320 (2013).

[53] Z. Kalaninová, A. N. Andreyev, S. Antalic, F. P. Heßberger, D. Ackermann, B. Andel, M. C. Drummond, S. Hofmann, M. Huyse, B. Kindler, J. F. W. Lane, V. Liberati, B. Lommel, R. D. Page, E. Rapisarda, K. Sandhu, Š. Šáro, A. Thornthwaite, and P. Van Duppen, Phys. Rev. C **87**, 044335 (2013).

[54] J. Uusitalo, J. Sarén, S. Juutinen, M. Leino, S. Eeckhaudt, T. Grahn, P. T. Greenlees, U. Jakobsson, P. Jones, R. Julin, S. Ketelhut, A.-P. Leppänen, M. Nyman, J. Pakarinen, P. Rahkila, C. Scholey, A. Semchenkov, J. Sorri, A. Steer, and M. Venhart, Phys. Rev. C **87**, 064304 (2013).

[55] A. N. Andreyev, D. Ackermann, S. Antalic, H. J. Boardman, P. Cagarda, J. Gerl, F. P. Heßberger, F. P. Heßberger, M. Huyse, M. Huyse, A. Keenan, H. Kettunen, A. Kleinböhl, A. Kleinböhl, I. Kojouharov, A. Lavrentiev, C. D. O'Leary, C. D. O'Leary, B. Lommel, M. Matos *et al.*, Eur. Phys. J. A **18**, 39 (2003).

[56] A. N. Andreyev, S. Antalic, D. Ackermann, T. E. Cocolios, V. F. Comas, J. Elseviers, S. Franchoo, S. Heinz, J. A. Heredia, F. P. Heßberger, S. Hofmann, M. Huyse, J. Khuyagbaatar, I. Kojouharov, B. Kindler, B. Lommel, R. Mann, R. D. Page, S. Rinta-Antilla, P. J. Sapple *et al.*, Phys. Rev. C **80**, 054322 (2009).

[57] P. Van Duppen, P. Decrock, P. Dendooven, M. Huyse, G. Reusen, and J. Wauters, Nucl. Phys. A **529**, 268 (1991).

[58] M. Huyse, E. Coenen, K. Deneffe, P. van Duppen, K. Heyde, and J. van Maldeghem, Phys. Lett. B **201**, 293 (1988).

[59] B. Andel, A. N. Andreyev, S. Antalic, M. Al Monthery, A. Barzakh, M. L. Bissell, K. Chrysalidis, T. E. Cocolios, J. G. Cubiss, T. Day Goodacre, N. Dubray, G. J. Farooq-Smith, D. V. Fedorov, V. N. Fedosseev, L. P. Gaffney, R. F. Garcia Ruiz, S. Goriely, C. Granados, R. D. Harding, R. Heinke *et al.*, Phys. Rev. C **102**, 014319 (2020).

[60] W. Q. Zhang, A. N. Andreyev, Z. Liu, D. Seweryniak, H. Huang, Z. H. Li, J. G. Li, C. Y. Guo, A. E. Barzakh, P. Van Duppen, M. Al Monthery, B. Andel, S. Antalic, M. Block, A. Bronis, M. P. Carpenter, P. Copp, J. G. Cubiss, B. Ding, D. T. Doherty *et al.*, Phys. Rev. C **106**, 024317 (2022).

[61] J. C. Batchelder, K. S. Toth, C. R. Bingham, L. T. Brown, L. T. Brown, C. N. Davids, T. Davinson, T. Davinson, R. J. Irvine, D. Seweryniak, W. B. Walters, P. J. Woods, J. Wauters, and E. F. Zganjar, Z. Phys. A Hadrons and Nuclei **357**, 121 (1997).